YUGATO

ISSN: 0387-5695, eISSN: 0387-5695
Vol. 75 No. 2 (2023)

Received: October 16, 2023 / Revised: November 11, 2023 / Accepted: December 09, 2023 / Published: December 30, 2023

INVESTIGATION INTO THE SITE-SPECIFIC BINDING INTERACTIONS BETWEEN L-TYROSINE AND CHLOROGENIC ACID USING MULTI-SPECTROSCOPIC AND MOLECULAR DOCKING STUDIES.

A.Kanimozhi and S.Bakkialakshmi a*
Department of Physics, Annamalai University, Annamalai Nagar,
Tamil Nadu, India
*Corresponding author email

Abstract

In this paper, UV- Vis spectroscopy, steady-state fluorescence, synchronous fluorescence spectra, Time-resolved fluorescence spectra, Fourier transform Infrared (FTIR), antibacterial activity, anticancer activity, and molecular docking analysis were used to investigate the mechanism of interaction between L-Tyrosine (L-TYR) and chlorogenic acid (CGA). Based on fluorescence quenching analysis, CGA quenched the inherent fluorescence of L-Tyrosine (L-TYR) remarkably through a static mechanism. Chlorogenic acid(CGA) is the common active phenolic acid in Chinese medicinal materials such as honeysuckle. It is a class of small molecules with multiple activities such as antioxidants, inhibiting cancer cells, lowering blood sugar, and lowering blood pressure. The simulated molecular docking showed that hydrophobic forces were also involved in the interaction between L-TYR and CGA. The conformation changes have been noted and the quenching mechanism between (L-TYR) and CGA proved to be static quenching by fluorescence.

Keywords: L-Tyrosine, Chlorogenic acid, Fluorescence, FTIR, Antibacterial activity, Anticancer activity, and Molecular docking.

1. Introduction

L- Tyrosine is a semi-essential amino acid to constitute the proteins, which was indispensable in human nutrition for establishing and maintaining a positive nitrogen balance [1]. It has been well known that amino acids are the main component element of various proteins. They generally play an important physiological role in the life process [2, 3]. Because of a special three-dimensional geometric configuration, all amino acids also exhibit the perfect identification and selection abilities for biological tissue [4, 5]. L-tyrosine is widely present in nature and is a building block of proteins. L-Tyrosine as an aromatic amino acid emits endogenous fluorescence. Fluorescence quenching of tyrosine has been utilized previously in a quantitative analysis [6, 7]. Tyrosine is an enzyme widely existing in plants, animal tissue, and fungi [8]. Mainly functions as catalyzing the hydroxylation of phenolic substrates to catechol derivatives, and further oxidizing the catechol derivatives as orthoquinone products. Additionally, this reaction has been proven a key point during the biosynthetic pathway of melanin and other natural pigments [9, 10]. However, the low sensitivity of traditional analyses for tyrosine has exhibited obvious limitations [11]. L- TYR is an essential aromatic amino acid and a vital constituent of proteins, which is indispensable in human nutrition for establishing and maintaining a positive nitrogen balance

[12, 13]. L- TYR can be synthesized in the body from phenylalanine; tyrosine is a precursor of neurotransmitters and hormones such as epinephrine, melanin, and thyroid hormones [14, 15]. TYR, through its effect on neurotransmitters, is used to treat, conditions including mood enhancement, appetite suppression, and growth hormone stimulation. Furthermore, tyrosine has an antioxidant ability [16].TYR plays significant roles in a biological system and it has been proven to be linked to various human diseases. Among them, L-Tyrosine is the precursor of dopamine, neurotransmitters, and thyroxin in mammalian central nervous systems, Parkinson's disease, depression, and other mood disorders were generally found when L-tyrosine levels were abnormal[17]. Recently, fluorescence analysis had become popular due to the advantages of fluorescence signaling and intrinsic sensitivity[18]. Although there have been numerous types of amino acid-based surfactants reported, the use of amino acids as building blocks for surfactants is still in its infancy. Amino acid-based surfactants, derived from arginine and lysine with high biodegradability and low toxicity profile have been reported to exhibit good antimicrobial activities [19, 20, 21]. Amino acid and their compounds with different metal ions play an important role in biology, pharmacy, and industry [22,23]. L-TYR is one of the 20 natural amino acids the molecule is interesting by its wide applications [24, 25]. Amino acids have been widely used in the production of agrochemicals, racemic drugs, fragrances, and pharmaceuticals [26]. The structure of L-Tyrosine has been shown in Fig 1

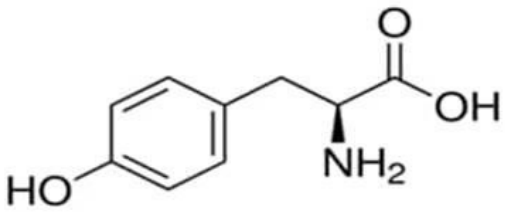

Fig. 1 Molecular Structure of L-Tyrosine

Polyphenols are a large class of secondary plant metabolites, widely distributed in the human diet such as fruit, vegetables, coffee, tea, chocolate, and beer [27]. Polyphenols have many biological activities, including powerful antioxidants which protect the body from damaging free radicals. [28].Experimental and epidemiological evidence has demonstrated that increased intake of polyphenols is associated with a reduced risk of cardiovascular disease and cancer [29,30]. Thus, daily intake of polyphenols is important for human health. Chlorogenic acid (CGA) is the most frequent form of phenolic compound in plants. The presence of the phenolic group enables it to act as a natural antioxidant, and it can bind to enzymes and other multisubunit proteins, modify their structural properties and alter their biological activities [31]. CGA is present in green coffee beans and citrus fruits, which are the best source of CGA found in plants with an amount of 5 -12g/100g.The structure of Chlorogenic acid has been shown in Fig 2.

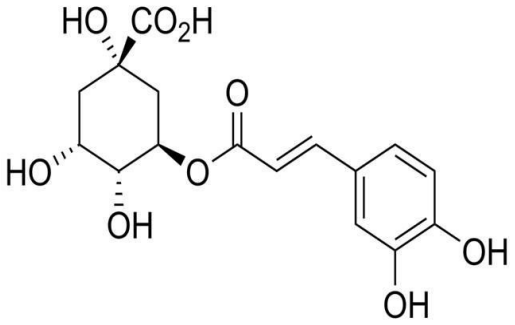

Fig. 2 Molecular structure of Chlorogenic acid

Chlorogenic acids are also used in the regulation of blood sugar and have the potential to aid the management of obesity[32,33]. The risk of type-2 diabetes decreased with increasing coffee consumption in which the CGAs are responsible for anti-diabetic activity[34,35]. As is known to all, fluorescent methods have attracted enormous attention and are widely distributed in many plants. As one of the most abundant polyphenols in people's daily diet, it is an important active ingredient in Chinese medicine [36]. Although the antioxidant properties of CGA are thought to reside in the catechol structure of the phenyl ring, the double bond conjugated with the catechol group may also serve as a site for free radical attack. Therefore, the stabilization of CGA is one of the most important concerns for its applications. It is a cinnamic acid of ester formed from caffeic acid and (-) - quinic acid [37].

The experimental studies, UV / Visible, Steady State fluorescence, Synchronous fluorescence, and time-resolved analysis assisted the conformation changes of L-TYR. The influences of the polyphenols on the secondary structure of protein were studied by FTIR, Molecular Docking, and Antibacterial activity for the polyphenol, CGA has also been carried out.

2 .Materials and Methods

L-Tyrosine reagent grade (≥ 98 %) and chlorogenic acid(≥ 95%) were purchased from Sigma-Aldrich Chemical Co. A stock solution L-TYR (10^{-4} M) was prepared with distilled water. The stock solution of chlorogenic acid (10^{-5} M) was prepared by using distilled water. The solutions were prepared just before taking absorption and fluorescence measurements

2.1 Spectroscopic instrument details

Absorption spectra were recorded between 200 to 400 nm with a SHIMADZU model (SHIMADZU 1800 PC UV/VIS spectrophotometer). Fluorescence spectra of each solution were recorded between 280 and 800 nm using an RF – 5301 PC (Shimadzu Corporation, Kyoto, Japan) fluorescence spectrophotometer. Fluorescence decay measurements were recorded using [Spectrofluometer make Jobin Yvon model fluoro-log – FL3 – 11 spectrofluometer]. FTIR spectra were recorded in a liquid sample of L-tyr with chlorogenic acid are measured from 4000-400 cm^{-1}[PerkinElmer model].

3 Results and discussion

3.1 UV –Visible spectroscopic study for L-TYR with chlorogenic acid

UV–vis spectroscopy is a simple and intuitive approach to investigating the structural changes in protein–ligand interactions[38]. UV –Visible absorption spectroscopy is a very simple yet important method for gathering knowledge on structural change and detecting the possibility of complex formation. The interactions of L-Tyrosine and Chlorogenic acid at different concentrations were studied using UV-Vis spectroscopy is shown in Fig 3.3.1.The increased absorption intensity peaks around 275 nm suggest the formation of complexes between L-TYR and CGA. The absorbance of L-TYR and CGA complexes was significantly elevated with increasing concentrations between 0.2 TO 1.0 M. This implies that CGA could lead to the modification of polarity and hydrophilicity of microenvironment around aromatic amino acid residues L-Trp, L-Tyr, and L-Phe of, which are responsible for changes of L-TYR and CGA conformation.

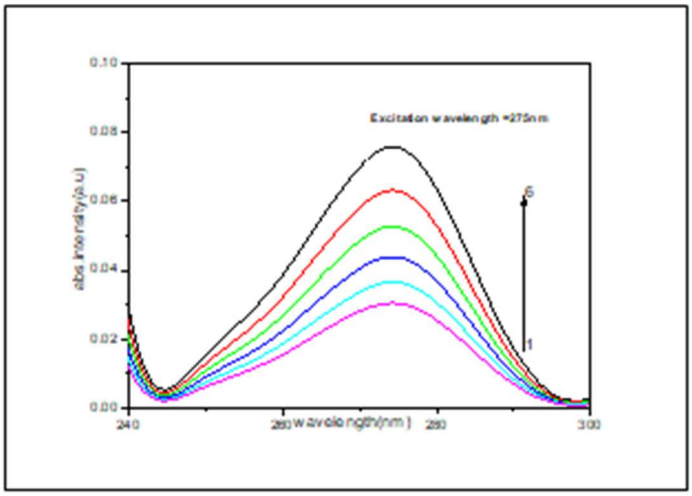

Fig. 3.1 UV/Vis absorption spectra of L-Tyrosine with different Concentration of CGA (mol L^{-1}) (1)0.0,(2)0.2,(3)0.4,(4)0.6,(5)0.8&(6)1.0

The binding constants of Chlorogenic acid with L-Tyrosine complexes were calculated by assuming that there is only one type of interaction between Chlorogenic acid and amino acid in an aqueous solution, the equations (3.14) and (3.15) can be established.

$$\text{L-TYR+ CGA} \rightleftharpoons \text{L-TYR: CGA} \qquad (3.14)$$

$$K = \frac{[\text{L-TYR: CGA}]}{[L-TY\ ][\text{CGA}]} \qquad (3.15)$$

Where K is the binding constant

Assuming, [L-TYR: CGA] = C_B

$$\text{K} = \frac{CB}{[L-TYR-\text{CB}\,][\,CGA-\text{C}\ ]} \qquad (3.16)$$

where $C_{L\text{-}TYR}$ and C_{CGA} are the analytical concentrations of L-TYR and CGA in solution respectively. According to Beer-Lambert's law

$$C_{L\text{-}TYR} = \frac{A_0}{\varepsilon_{L-TRP}.l} \qquad (3.17)$$

$$C_B = \frac{A-A_0}{\varepsilon_B.l} \qquad (3.18)$$

where, A0 and A are the absorbance of L-TYR in the absence and presence of CGA respectively. $\varepsilon_{L\text{-}TYR}$, ε_B is the molar extinction coefficients of L-TYR and the bound CGA , respectively. l is the light path of the cuvette (1cm).

By displacing in the equation (3.16) by equations (3.17) and (3.18), Eqn (3.19) can be deduced:

$$\left[\frac{A}{A-A_0}\right] = \left[\left(\frac{\varepsilon_{L-TYR}}{\varepsilon_B}\right) + \left(\left(\frac{\varepsilon_{L-TYR}}{\varepsilon_B}\right).k\left(\frac{1}{(C_{CGA})}\right)\right)\right] \qquad \textbf{(3.19)}$$

Thus, the double reciprocal plot of $\frac{1}{A-A_0} Vs \frac{1}{(C_{CGA})}$ is linear and the binding constant [K] can be estimated from the intercept to the slope ratio.

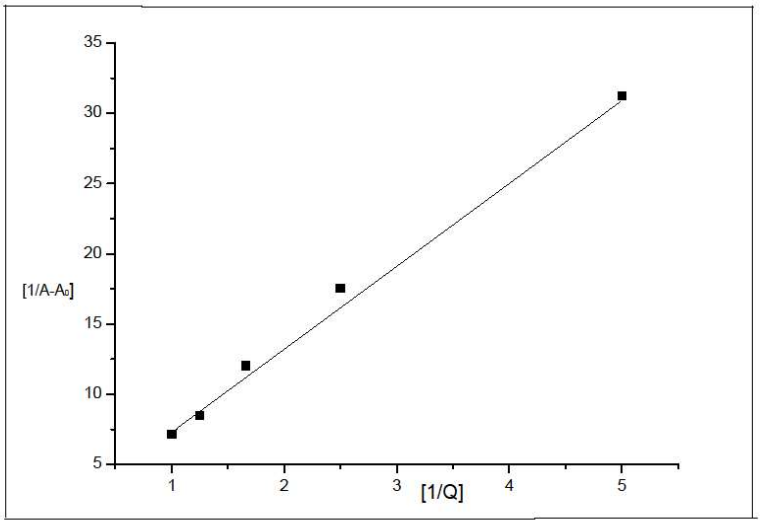

Fig. 3.2: Double reciprocal Plot of $\left[\frac{1}{A-A_0}\right]$ versus $\left[\frac{1}{[Q]}\right]$ for L-Tyrosine and CGA

3.2Fluorescence quenching of L-Tyrosine with Chlorogenic acid

Fluorescence quenching of protein can provide useful information on Chlorogenic acid–L-TYR binding. Fig. 3.3.3 showed the fluorescence quenching spectra of L-TYR induced by different concentrations CGA [39]. Fluorescence quenching of L-TYR shows the change in fluorescence emission spectra with different concentrations of chlorogenic acid. The slit widths for the excitation and emission monochromators were set to 5 nm, respectively, and 600 scans were acquired per minute. From the spectrum, it was clear that the fluorescence intensity of L- TYR decreases at around 306 nm with increasing the concentration of chlorogenic acid.

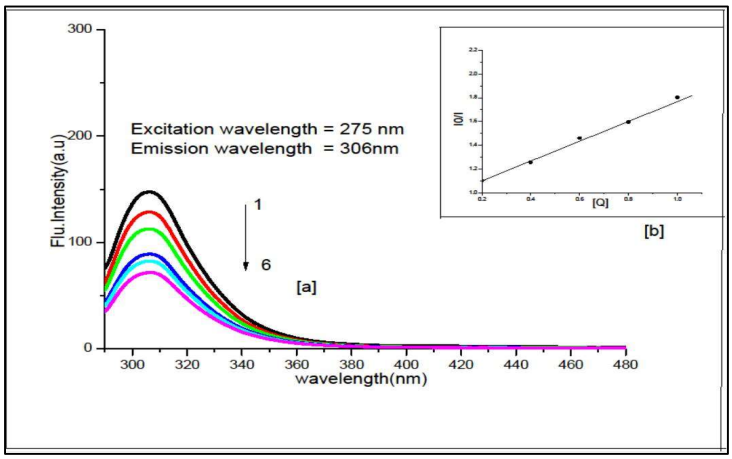

Fig.3.3: (a) Steady-state fluorescence spectra of L-Tyr with Different concentrations of chlorogenic acid (mol L^{-1})(1)0.0,(2)0.2,(3)0.4,(4)0.6 (5)0.8&(6)1.0

(b) Stern-Volmer plot of L-TYR with CGA

The fluorescence emission of L-TYR was quenched by chlorogenic acid with no spectral shift and indicating that interactions with chlorogenic acid do not influence the environment of fluorophores in amino acid. Fluorescence intensity can be decreased by a wide variety of processes called quenching reactions; the compounds causing them are called quenchers. This suggested that the interaction of L-TYR with chlorogenic acid caused fluorescence quenching and changes in the microenvironment of the fluorophores. The fluorescence quenching can be divided into static quenching and dynamic quenching connected to the binding. For, dynamic and static quenching Stern- Volmer constant K_{SV}, an important parameter to distinguish the quenching mechanism, increases and decreases with the increase of concentration respectively.

$$F_0 = 1+K_{sv}\,[Q] = 1+ K_q\tau_0[Q] \qquad \textbf{(3.20)}$$

Where F_0 and F denote the steady-state fluorescence(L-TYR) intensities in the absence and the presence of the quencher chlorogenic acid respectively. K_q is the biomolecular quenching rate constant,τ_0 is the average lifetime of the amino acid,[Q] is the concentration of the quencher, and K_{sv} is the stern –Volmer quenching

constant. The above equation is applied to determine K_{sv} by linear regression of a plot of (F_0/F) against [Q].

The classical Stern – Volmer plot of L-TYR in the presence of CGA is shown in Fig.3.3(b) The stern-Volmer quenching constant and biomolecular quenching rate constant (K_q) are shown in Table3.1.

Table3. 1: Stern – Volmer (K_{sv}) and biomolecular quenching rate constant (K_q) of L-TYR with CGA

Quencher	$K_{SV}\times 10^{-5}$ (L mol^{-1})	K_q (L $mol^{-1}s^{-1}$)	R[a]	S.D[b]
CGA	0.78	4.45×10^{13}	0.98	0.76

[a] → is the correlation coefficient, [b] → is the standard deviation

3.3 Binding constant and number of binding sites

When small molecules bind independently to a set of equivalent sites on a macromolecule and the equilibrium between the free and the bound molecules has been reached, the fluorescence intensities obey the following equation[40]. It is assumed that there are identical and independent sites in biological molecules for the static quenching mechanism.

$$\text{Log } (F_0 - F)/F = \log K_a + n \log [Q] \qquad \textbf{(3.21)}$$

Where K_a is the binding constant and n is the number of binding sites per L-Tyrosine molecules and [Q] is the quencher concentration. This is shown in Fig.3.3.4.

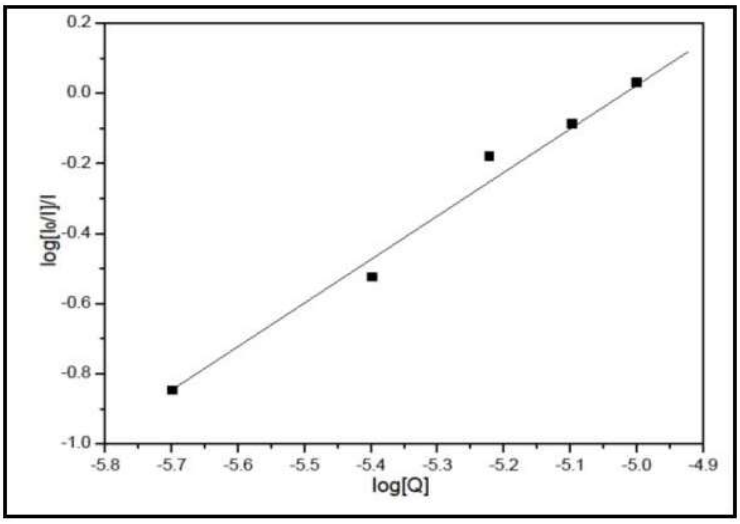

Fig. 3.4. Double log plot of L-Tyrosine with chlorogenic acid

Table 3.2.The binding constant (K_a), binding site (n) and correlation coefficient (R) of L-Tyrosine with CGA

Quenchers	K_a x 10^6 (L mol^{-1})	n	R
L-TYR+CGA	1.7354	1.0730	0.9862

3.4 Mechanism of quenching

The quenching of L-Tyrosine can be explained by several possible mechanisms such as electron transfer, energy transfer, proton transfer or hydrogen atom transfer. Fig.3.3.5. shows the fluorescence emission spectra of L-TYR with various quantities of CGA following excitation at 275 nm. It can be seen from the figure that the fluorescence intensity of L-TYR decreases steadily and with the addition of CGA, there is almost no shift in the emission wavelength (λ_{emi}=306nm). Under the same conditions, no fluorescence of CGA was observed. These results simply shows that the interaction between CGA and L-TYR occurs resulting in the quenching of the intrinsic fluorescence of L-TYR. Fluorescence intensity of L-TYR was observed to decrease steadily; for the emission wavelength with increasing concentration of the drug, indicating the formation of a quencher-fluorescer complex. Essentially, there exists four types of non-covalent interactions in the binding of the ligands to protein. These are hydrogen bonds, Van Dar Waals forces, hydrophobic and electrostatic interactions. Thermodynamic parameter, ΔG, , binding constant (K) can be evaluated using the following equation(3.9)

$$\Delta G = - RT \ln K. \qquad (3.22)$$

The negative sign for ΔG means that interaction is spontaneous. The calculated ΔG values (ΔG_g–ground state, ΔG_e–excited state) are given in Table 3.4

3.5 Synchronous fluorescence Spectroscopy

The synchronous fluorescence spectra can provide the characteristic information of tyrosine residues or tryptophan residues in L-TYR when the $\Delta\lambda$ between excitation and emission wavelength is set at 15 or 60 nm, respectively. The effect of phenols on the conformational changes of L-$_{TYR}$ can be investigated by synchronous fluorescence spectroscopy**[41].**Some changes in the microenvironment around the L-TYR fluorophore can be reflected through the synchronous fluorescence scanning. In synchronous fluorescence spectra, the shift in the maximum λ_{em} reveals the alteration of the polarity microenvironment near the Tyr and Trp residues when $\Delta\lambda$ was set as 15 and 60 nm, respectively. No significant shift occurred at $\Delta\lambda$ = 15 nm, and 60 nm (the synchronous fluorescence spectra are shown in Fig.3.3.5), indicating that the interactions of CGA–L-TYR slightly affected the protein conformation of the region around Trp residues, as analyzed from the fluorescence emission spectra. The same conclusion was obtained in a Moreover, the regular decrease in fluorescence intensity with ligand addition (Fig. 3.5) again demonstrated the occurrence of fluorescence quenching during binding.

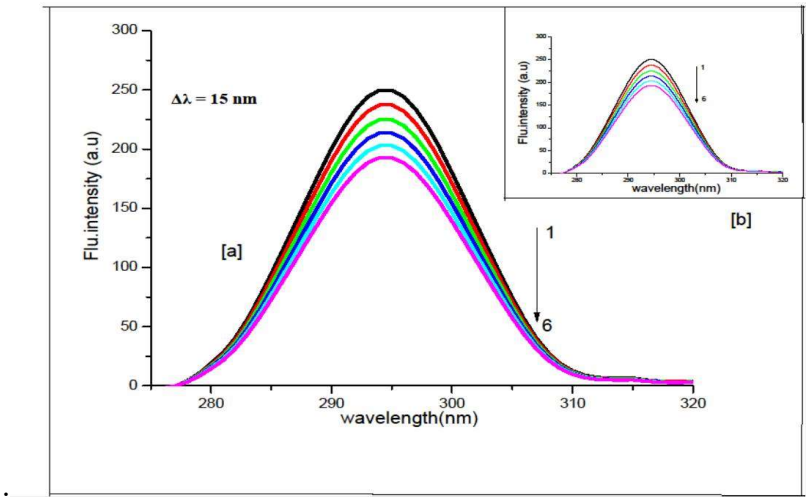

Fig.3.5 Synchronous fluorescence spectra for L-Tyrosine with chlorogenic acid having $(\boldsymbol{a})\Delta\boldsymbol{\lambda}$ = 15nm (b)$\Delta\boldsymbol{\lambda}$ = 60nm

In this work, the ratios of synchronous fluorescence quenching were used to determine the binding sites of CGA to L-tyrosine molecules. As the concentration of CGA increased, the fluorescence intensity of L-TYR at $\Delta\lambda$ =15nm and $\Delta\lambda$ = 60nm decreased with no spectra shift occurring. This phenomenon demonstrated that CGA induced tertiary structural changes in the microenvironment of L-tyrosine residue at the interface, from a hydrophilic to a hydrophobic environment.

3.6 Fluorescence lifetime measurements of L-TYR with CGA

Time-resolved measurements reveal whether quenching is due to diffusion or too complex formation with the ground state fluorophores. In fluorescence, much of the molecular information content is available only by time-resolved measurements.Time–resolved fluorescence is a very precise technique to distinguish between static and dynamic quenching. According to the theory of Lakowicz, [42].Fluorescence quenching is preferably acquired by time-resolved fluorescence measurements, which can distinguish between static and dynamic processes immediately. The measurement of fluorescence lifetimes is the most definitive method to distinguish static and dynamic quenching This is shown in Fig 3.6.

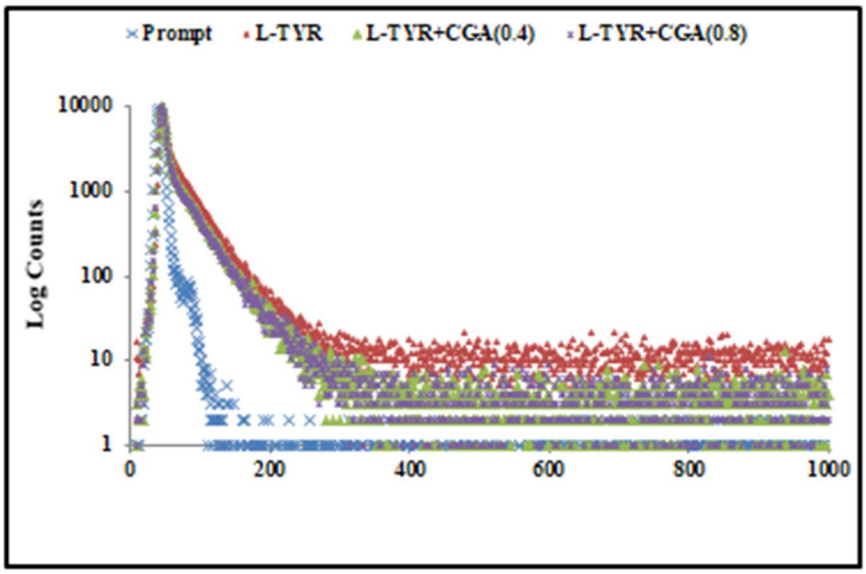

Fig. 3.6: Time-resolved fluorescence spectra of L-Tyrosine with different Concentrations of CGA(mol dm^{-5}) (1) 0.0, (2) 0.4, and (3) 0.8

Therefore, the quenching mechanisms for the interaction of Chlorogenic acid with L-Tyrosine were further confirmed through lifetime measurements. The time-resolved decay curves of L-Tyrosine in the absence and presence of flavonoids were shown in Fig3.3.6. The decay curves fitted well to a bi-exponential function; the relative fluorescence lifetime is τ_1 =3.03 ns, τ_2 = 5.48 ns, and τ_3 = 1.45 ns (χ2 = 1.01) of L-TYR, whereas, in the maximum concentration of CGA, the lifetime is τ_1 =2.43ns, τ_2 =4.60 ns and τ_3 = 6.68 ns. The data fit well to the sum of a single exponential decay with a $\boldsymbol{\chi}^2$ value close to 1.15. The decay parameters for all the systems were summarized in Table 3.5. As illustrated in Fig3.3.6. there is no obvious difference in the decay curves of L-Tyrosine with increasing amounts of CGA . The average lifetime ($\boldsymbol{\tau}$) for biexponential interactive fittings was calculated from decay times and the relative amplitude ($\boldsymbol{\alpha}$) using the following equation.

$$<\tau> = \frac{\tau_1\alpha_1^2+\tau_2\alpha_2^2+\tau_3\alpha_3^2}{\tau_1\alpha_{1+}\tau_2\alpha_{2+}\tau_3\alpha_3} \qquad \textbf{(3.23)}$$

The average fluorescence lifetime decreased from 1.76 ns and 0.90 ns without and with the CGA, attesting that the fluorescence quenching here is fundamentally a static mechanism. Table 3. Presents the fluorescence lifetime values of L-TYR without and with different concentrations of CGA. For static quenching, the fluorescence lifetime of fluorophore will not disturb during the complex formation. Consequently, a conclusion may be safely drawn that the quenching mechanisms of L-Tyrosine with CGA all belong to static quenching with complex formation.

Table 3.3: Fluorescence lifetime and relative amplitudes of L-TYR with different centrations of CGA

Concentration (M)	Lifetime (ns)	Average	Relative amplitude	x^2	S.D× 10^{-11} sec

	τ_1	τ_2	τ_3	lifetime $\times 10^{-9}$ Sec	B_1	B_2	B_3		τ_1	τ_2	τ_3
L-TYR	3.03	5.48	1.45	1.76	32.75	12.60	54.65	1.01	1.32	1.66	1.57
LTYR+CGA(0.4)	2.65	4.81	6.25	0.90	12.04	11.17	76.79	1.13	1.77	9.78	1.06
L-TYR+CGA (0.8)	2.92	5.15	5.32	0.75	10.97	6.80	82.24	1.20	2.50	1.42	1.20

3.7. Fluorescence Resonance Energy Transfer between CGA and L-TYR

Energy transfer efficiency (E), average binding distance (r) and critical distance with efficiency transfer of 50% (R_o) can be calculated based on fluorescence resonance energy transfer (FRET) theory according to following formula[43]..In conventional FRET, the energy is transferred nonradiatively from an excited donor molecule to an acceptor in ground state via an induced dipole–dipole interaction.The overlap of the UV absorption spectrum of CGA with the fluorescence emission spectrum of L-Tyrosine is shown in Fig. 3.7.

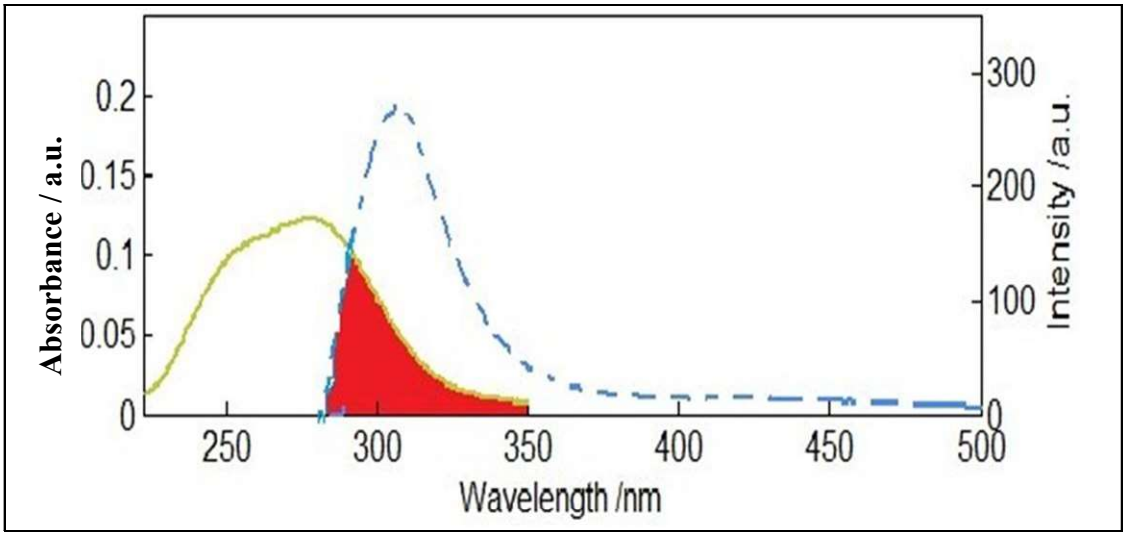

Fig.3.7 The overlap of UV absorption spectra of CGA (solid line) with the fluorescence emission spectra of L-Tyrosine (dotted line)

The spectral studies suggested that CGA interacted with L-Tyrosine. The distance, r between the in L-Tyrosine and the bound CGA could be determined using FRET. However, the r-value is calculated for CGA with L-Tyrosine. The efficiency of energy transfer, E, is calculated using the equation.

$$E = 1- F/F_O = R_0^6/R_0^6+r_0^6 \quad \textbf{(3.24)}$$

Where F and F_0 are the fluorescence intensities of L-Tyrosine in the presence and absence of CGA, and R0 is the critical distance when the transfer efficiency is 50 %. The average distance between the donor and acceptor is denoted by r. J is the overlap integral of the fluorescence emission spectrum of the donor and absorption spectrum of the acceptor and it was calculated using the overlapped component of the L-TYR emission spectrum and CGA absorption spectrum, and it was $8.11 \times \mathbf{10^{-15} cm^{-3}\ M^{-1}}$. Furthermore, the E, R_O, and r values were 2.51 nm and 2.34 nm, respectively. Since the distance between L-TYR and CGA was 8nm indicates .the energy transfer from L-TYR with CGA exists with a high probability.

3.8 FTIR spectroscopic study of L-Tyrosine with Chlorogenic acid

FTIR spectroscopy was an important technique to investigate the chemical compounds and functional groups of protein hydrolysates. Fourier transform infrared spectroscopy can be used to provide information about changes in the secondary structure of the protein. several characteristic peaks were obtained for L-Tyrosine, which could be related to the presence of specific functional groups In this study, amide I, II, and III were evaluated. This is shown in Fig 3.3.8.

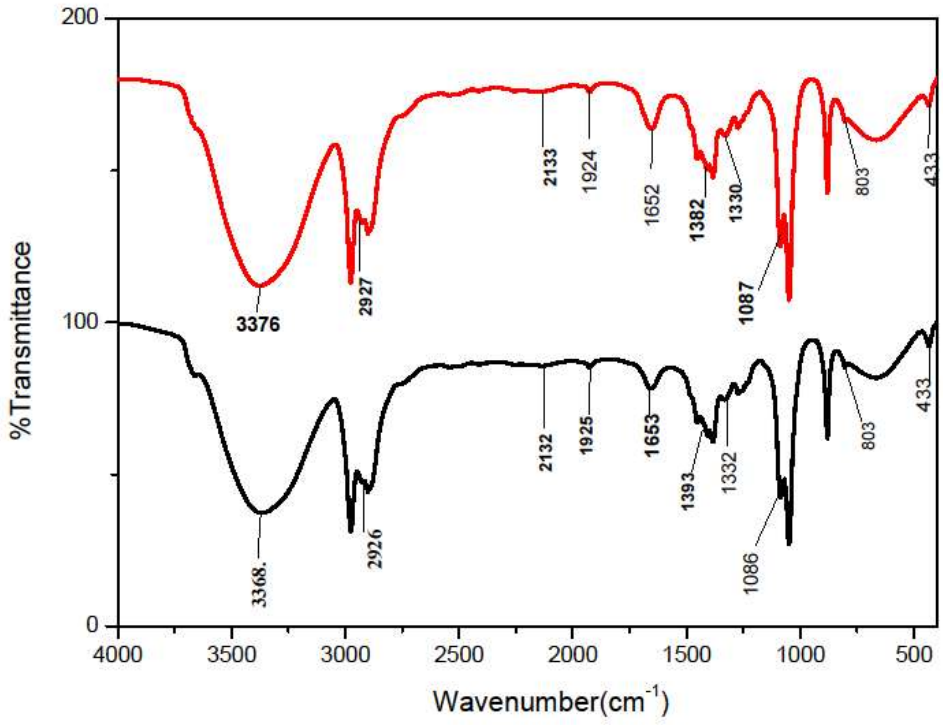

Fig.3.8 FTIR spectra of (a)L-TYR,(b)L-Tyrosine with CGA

The infrared spectra were recorded on Fourier transform spectrometer in the mid-infrared region (MIR) within the range of 400-4000$\boldsymbol{cm^{-1}}$. Because of the complex interaction of atoms within the

molecule, IR absorption of the functional groups may differ over a wide range of the FTIR bands at 4000 - 1450 $\boldsymbol{cm^{-1}}$ represents functional group region, the appearance of robust abruption bands in the region of 4000 to 2500 $\boldsymbol{cm^{-1}}$ was because of stretching vibrations between hydrogen and some additional atoms with a mass of 19 (or) less.

The spectra of L-Tyrosine feature a broad and intensive band around 3368 cm^{-1} peak shift to 3376 cm^{-1} maybe due to the interaction of hesperidin with the OH band of L-Tyrosine. The spectra of L-Tyrosine 2926 cm^{-1}peak shifted to 2927 cm^{-1}C-H stretching. The spectra L-TYR 2132cm^{-1} peak shifted to 2133 cm^{-1} C=C stretching. The spectra of L-TYR 1925 cm^{-1} peak shifted to1924 $cm^{-1}\mathrm{C}=\mathrm{C}=\mathrm{C}$ stretching. The spectra of L-TYR 1653cm^{-1} peak shifted to 1652cm^{-1} C=N stretching. The spectra of L-TYR 1393 cm^{-1}peak shifted to 1382 cm^{-1} C-N Stretching. The spectra of L-TYR 1332 cm^{-1}peak shifted to 1330 cm^{-1}C-N Stretching. The spectra of L-TYR 1 273cm^{-1}peak shifted to 1274 cm^{-1}C-O Stretching. The spectra of L-TYR 1086 cm^{-1}peak shifted to 1087 cm^{-1}C-N Stretching.

Table 3.4 FTIR peak assignment of L-TYR without and with different concentrations of CGA

Wavenumber cm^{-1}		**Tentative Peak assignment**
L-TYR	**L-TYR+CGA**	
3368	3376	O – H Stretching
2926	2927	C-H Stretching
2132	2133	C=C Stretching
1925	1924	C=C=C stretching
1653	1652	C=N Stretching
1393	1382	C-N Stretching
1332	1330	C-N Stretching
1086	1087	C- N Stretching

3.9 ANTIBACTERIAL ACTIVITY STUDY FOR L-TYROSINE WITH CHLOROGENIC ACID

All complexes were tested for antibacterial activity against both Gram-positive (Staphylococcus aureus) and Gram-negative (Escherichia coli) bacteria. The antibacterial function of complexes, represented as the diameter of the growth-inhibition region in millimetres, is shown in (Fig.6.2.2). The antibacterial activity is one of the most remarkable properties of marine phenolics and has been widely studied. The qualitative antibacterial assay of the samples was carried out by the agar diffusion method Bacteria have a great capacity for adjusting their metabolism in response to environmental changes by linking extracellular stimuli to the regulation of genes by transcription factors and in certain cases, transcription regula*tors* control genes and operons that belong to different metabolic pathways

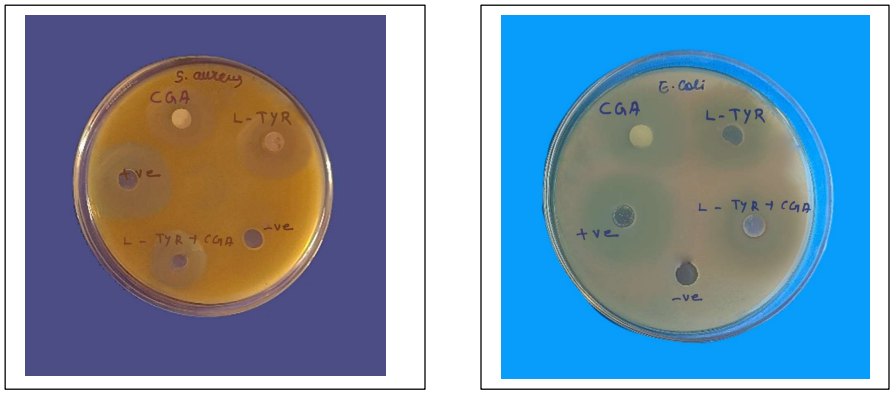

Fig. :3.9 The antibacterial activity of CGA,L-TYR, and L-TYR+CGA

Table 3.5: Antibacterial activity of L-TYR and Chlorogenic acid

S.NO	Bacterial Pathogens	Zone Of Inhibition (mm)				
		CGA	L-TYR	L-TYR+CGA	Positive control	Negative control
1	**Staphylococcus aureus**	21mm	22mm	23mm	30mm	-
2	**Escherichia coli**	20mm	19mm	18mm	28mm	-

Table 3.5 shows S. aureus (21 mm,22mm, and 23nm) and E.coli (20mm,19mm, and 18nm),and positive control of S.aureus and E.coli (30mm and 28mm). S.aureus and showed a higher antibacterial effect on Gram-positive bacteria than on Gram-negative bacteria. Finally, Antibacterial activity shows potent against both gram-positive and gram-negative bacteria. Compared with S.aureus and E.coli showed better antibacterial effect and stronger action intensity to cell wall and membrane, so as to achieve a better antibacterial effect.

3.10 MOLECULAR DOCKING STUDIES ON CHLOROGENIC ACID WITH TWO ANTIBACTERIAL PROTEINS

To investigate the relationship and free energy of these ligands' binding to the protein.Calculating the leading binding modes of the ligand and the three-dimensional protein structure is made easier with the help of the well-organized method known as molecular docking. Predicting binding modes is essential for identifying important structural characteristics and interactions as well as for providing information that may be used to create efficient inhibitors A well-established method for figuring out how two molecules interact and ligand orientation that would result in a complex with the lowest overall energy is called molecular docking studiesThe experimental crystal structures of the proteins, Tryptophanyl-tRNA Synthetase from *Escherichia coli* (PDB code 5V0I) and Tyrosyl-tRNA synthetase from *Staphylococcus aureus* (PDB code 1JIJ) were prepared utilizing UCSF Chimera 1.17.3 software (Pettersen et al., 2004). The energy minimized Tryptophanyl-tRNA Synthetase from *Escherichia coli* and Tyrosyl-tRNA synthetase from *Staphylococcus aureus* were docked with Chlorogenic Acid. The Protein Data Bank (PDB) was used to derive the

first three-dimensional [3D] structures for S. aureus ATCC 25923 (PDB id: 1JIJ), E. coli ATCC 25922 (PDB id: 5V0I)), and chlorogenic acid.During docking, auto dock tools and auto dock vina software were utilized. The docking figure i.e., the 3D structural view is shown in Fig.3.10. (a) and (b). For discussion, the first docked conformations have been chosen in each case because it poses minimum energy. The data are given in Tables 7.1

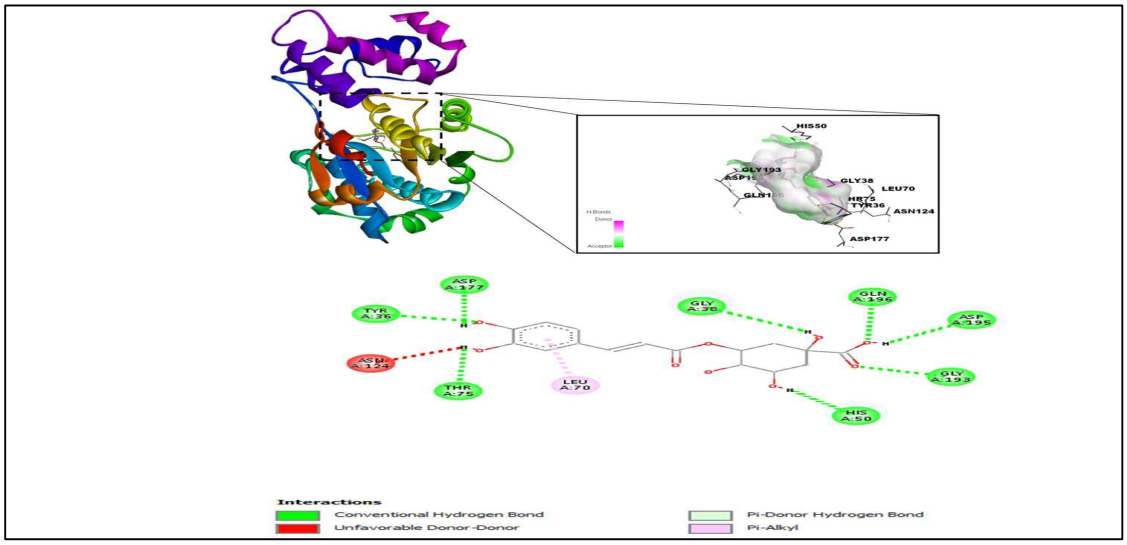

Fig.3.10 (a) Docked complex of Tyrosyl-tRNA synthetase from Staphylococcus aureus with chlorogenic acid (b) 2D Interaction Plot of Docked Complexe of Tyrosyl-tRNA synthetase from Staphylococcus aureus with chlorogenic acid

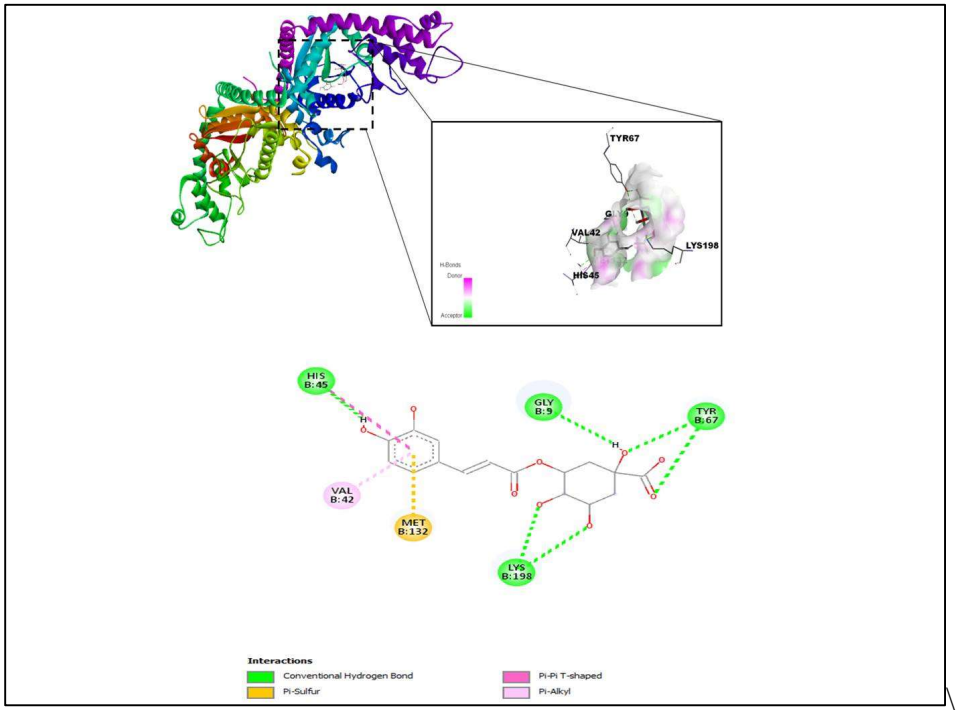

Fig.3.10,1(a).Docked complex of Tryptophanyl-tRNA Synthetase from Escherichia coli with chlorogenic acidm(b) 2D Interaction Plot of

Docked Complexe of Tryptophanyl-tRNA Synthetase from Escherichia coli with chlorogenic acid

The binding pattern was maintained despite a range of root mean square deviation (RMSD) values between 1 and 2. The grid map points for S. aureus and E. coli with CGAwere 23 and 23 and 23 respectively. By searching for the best active regions for protein-ligand interactions, we hope to identify the hydrogen binding interactions that take place between ligand-receptor complexes.The population size in this case was about 150, and the maximum number of generations was roughly 27000. The Lamarckian genetic algorithm (LGA) was applied. Docking results against s.aureus with CGA and e.coli with CGA, The protein revealed a binding area that was well-conserved, while the best binding energy value was only marginally expected**.**The calculated binding energy and the inhibition constant values are presented in Table 3.6

Table.3.6.Binding energyΔe (kcal/mol), and rmsd (å) of s.aureus, e.coli with CGA

PDB code	**Biological source**	**Protein name**	**RMSD Å**	**Binding Energy Δ E (kcal/mol)**
1JIJ	Staphylococcus aureus	Tyrosyl-tRNA synthetase (TyrRS)	3.2	-9.1 kcal/mol
5VOI	Escherichia coli	Tryptophanyl-tRNA Synthetase	1.90	- 7.7 kcal/mol

Compounds S. aureus with CGA (-9.1 kcal/mol) and E. coli with CGA (-7..7 kcal/mol) had the best free binding energies. The above information indicated that the stabilization at the binding cavity of S.aureus with CGAand e.coli with CGA complex was mostly due to residues as shown in the table.7.1.TYR A:36, GLY A:38, HIS A:50, LEU A:70, TYR A:75, ASN A:124, ASP A:177, GLY A:193, GLN A:196 and GLY B:9, VAL B:42, HIS B:45, TYR B:67, MET B:132, LYS B:198.The hydrogen bond between the active site residue of S.aureus with CGA and E.coli with CGA was also noted for interaction analysis.

3.11 ANTICANCER ACTIVITY STUDY ON CHLOROGENIC ACID

One of the most prevalent polyphenolic substances in the human diet is chlorogenic acid (CGA), which is an ester in which the hydroxyl group at position 5 of quinic acid (5-O-caffeoylquinic acid) is bonded to the acidic portion of caffeic acid. CGA belongs to a group of phenolic compounds produced by some plant species and is an important metabolite of coffee, the amount of which ranges from 70 to 350 mg in a 200 mL cup of coffee.Epidemiological studies have reported that CGA shows many biological properties, including antioxidant, anti-inflammatory, antiviral, and anticancer activities, and may be responsible for the reduced risk of some chronic diseases.

Cervical cancer is characterized by the rapid and uncontrolled growth of abnormal cells on the cervix. The concentration of phytochemicals plays a role in their cytotoxicity and anticancer property. Probably, at higher concentrations, phytochemicals exhibit prooxidant properties and this pro-oxidant property might disrupt cellular activity. This might be the reason for the increased cytotoxicity at higher doses. The human cervical cancer cell line (HeLa) was plated separately using 96 well plates with a concentration of 1×104 cells/well in MEM media with 1X Antibiotic Antimycotic Solution and 10% fetal bovine serum (Himedia, India) in a CO_2 incubator at 37˚C with 5% CO2. The cells were washed with 200 µL of 1X PBS, then the cells were treated with various test concentrations of a sample (CHL) and with IC50 concentration of Doxorubicin (12 µg/ml) as a positive control in serum-free media and incubated for 24 h. The medium was aspirated from cells at the end of the treatment period. 0.5mg/mL MTT prepared in 1X PBS was added and incubated at 37˚C for 4 h using CO2 incubator. After the incubation period, the medium containing MTT was discarded from the cells and washed using 200 µL of PBS. The formed crystals were dissolved with 100 µL of DMSO and thoroughly mixed. The development of color intensity was evaluated at 570nm. The formazan dye turns purple and blue color. The absorbance was measured at 570 nm using a microplate reader. The proliferation of HeLa cells was significantly inhibited by CHL in a concentration-dependent manner. The results of the anticancer activity test on chlorogenic acid in HeLa cervical cancer cells are presented in Fig .8.2 (a) &(b).

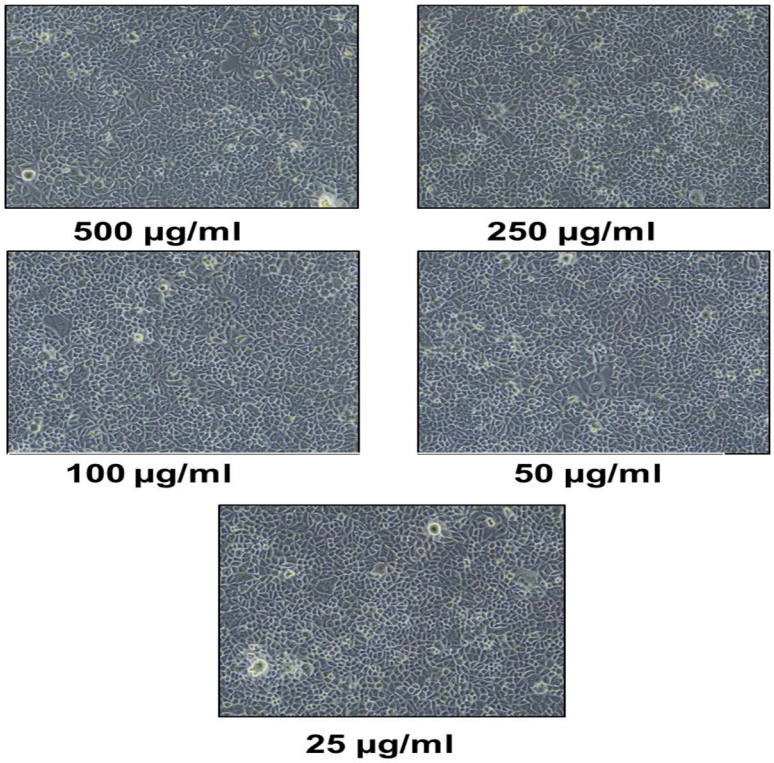

Fig.3.11(a) & (b) Effect of chlorogenic acid different concentrations on cell viability microscopic image of HeLa cell.

The anticancer efficiency chlorogenic acid compound was human cervical cancer cell line (HeLa) and the effect of cytotoxicity on the cancer cell line was evaluated MTT assay method. The anticancer on the cervical cancer cell line was a different concentration of sample loading (25,50,100,250, and 500 µg/ml) shown in Fig.8.2.The graph shows that there is a positive relationship between the log concentration of the ethanol and extract and the percentage of inhibition of HeLa cervical cancer cells. it means that the higher the log concentration, the higher percentage of inhibition on HeLa cells. Therefore the largest concentration of inhibition, using 500 µg/ml.

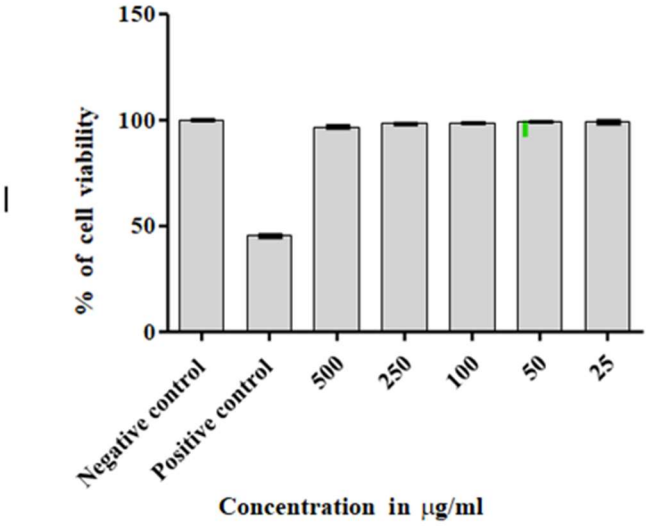

Fig.8.2(b) concentration versus cell viability

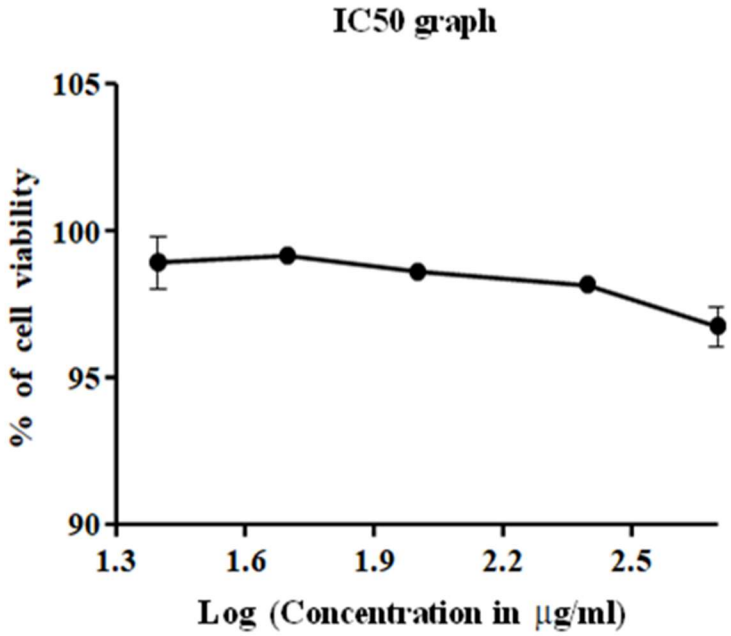

The anticancer activity of chlorogenic acid was exhibited by their anticancer effect on the HeLa cell line and the anticancer efficiency of the sample was expressed by IC_{50} value was The anticancer activity which is observed by the morphological image analysis is shown in Fig.. IC50 > 500 µg/ml.Besides ,while the concentration increases,the cytotoxicity increases leading to the death of cells and distinguished in a cervical cancer cell line.

3.11 Conclusion

In this present study,multi-spectroscopic techniques were used to explore the interaction between L-Tyrosine and chlorogenic acid. The results show that both L-Tyrosine and CGAhad a great influence on intrinsic fluorescence, UV absorption spectroscopy, synchronous spectroscopy, FTIR, FRET, antibacterial activity, anticancer activity, and molecular docking. Which are indicative of the types of interactions between CGA and L-Tyrosine.Moreover, the analysis of the fluorescence quenching data shows that the binding process of the complex is spontaneous. The main interaction forces between L-Tyrosine and S.aureus with E.coli are hydrogen bonding and van der Waals force. However, the hydrophobic interaction is the major interaction force between L-Tyrosine and s.aureus with e.coli.Thus, the present study can partly some insight into our understanding of the mechanism involved in the application of polyphenols in the preservation of aquatic products. These results may provide a basis for the combined application of L-Tyrosine and CGA in food and medicine.

Funding

No funding was received for this work

Declaration of competing interest

The authors declare that they have no conflict of interests.

Ethical approval

Ethics approval was not required for this research.

Informed consent statement

Not applicable

Author contribution

A.Kanimozhi written the manuscript and Dr.S.Bakkialakshmi review the manuscript

Data Availability Statement

The authors confirm that all behavioral data to support the findings of our study are available in the paper.

References

1. Jin, G. P., & Lin, X. Q. (2004). The electrochemical behavior and amperometric determination of tyrosine and tryptophan at a glassy carbon electrode modified with butyrylcholine. *Electrochemistry communications*, *6*(5), 454-460.

2. Zhang, Y., Jin, Y., Williams, T. A., Burtenshaw, S. M., Martyn, A. C., & Lu, R. (2010). Amino acid deprivation

induces CREBZF/Zhangfei expression via an AARE-like element in the promoter. *Biochemical and biophysical research communications*, *391*(3), 1352-1357.

3. Errico, F., Napolitano, F., Nistico, R., Centonze, D., & Usiello, A. (2009). D-aspartate: an atypical amino acid with neuromodulatory activity in mammals. *Reviews in the Neurosciences*, *20*(5-6), 429-440.

4. Shiratori, M., Kobayashi, T., & Shibui, T. (2009). Identification of amino acids essential for antibody binding by mRNA-display using a random peptide library: an anti-human tumor protein p53 antibody as a model. *Molecular biotechnology*, *41*, 99-105.

5. Mazumder, R., Hu, Z. Z., Vinayaka, C. R., Sagripanti, J. L., Frost, S. D., Kosakovsky Pond, S. L., & Wu, C. H. (2007). Computational analysis and identification of amino acid sites in dengue E proteins relevant to development of diagnostics and vaccines. *Virus Genes*, *35*, 175-186.

6. Gan, X. J., Liu, S. P., Liu, Z. F., Hu, X. L., Tian, J., & Xue, J. X. (2013). Fluorescence quenching method for the determination of carbazochrome sodium sulfonate with aromatic amino acids. *Luminescence*, *28*(3), 265-269.

7. Gan, X., Liu, S., Liu, Z., & Hu, X. (2012). Determination of tetracaine hydrochloride by fluorescence quenching method with some aromatic amino acids as probes. *Journal of fluorescence*, *22*, 129-135.

8. Wang, C., Yan, S., Huang, R., Feng, S., Fu, B., Weng, X., & Zhou, X. (2013). A turn-on fluorescent probe for detection of tyrosinase activity. *Analyst*, *138*(10), 2825-2828.

9. Ichikawa, A., Takagi, H., Suda, K., & Yao, T. (2009). New Methodological Approach for the Rapid and Sensitive Detection of Melanocytes and Melanocytic TumoursThe DOPA-GA Method. *Dermatology*, *219*(3), 195-201.

10. Li, S., Mao, L., Tian, Y., Wang, J., & Zhou, N. (2012). Spectrophotometric detection of tyrosinase activity based on boronic acid-functionalized gold nanoparticles. *Analyst*, *137*(4), 823-825.

11. Gauillard, F., Richardforget, F., & Nicolas, J. (1993). New spectrophotometric assay for polyphenol oxidase activity. *Analytical Biochemistry*, *215*(1), 59-65.

12. Chitravathi, S., Swamy, B. K., Mamatha, G. P., & Chandrashekar, B. N. (2012). Electrocatalytic oxidation of tyrosine at poly (threonine)-film modified carbon paste electrode and its voltammetric determination in real samples. *Journal of Molecular Liquids*, *172*, 130-135.

13. Weber, F. L., & Reiser, B. J. (1982). Relationship of plasma amino acids to nitrogen balance and portal-systemic encephalopathy in alcoholic liver disease. *Digestive Diseases and Sciences*, *27*, 103-110.

14. Jin, G. P., & Lin, X. Q. (2004). The electrochemical behavior and amperometric determination of tyrosine and tryptophan at a glassy carbon electrode modified with butyrylcholine. *Electrochemistry communications*, *6*(5), 454-460.

15. Currie, P. J., Chang, N., Luo, S., & Anderson, G. H. (1995). Microdialysis as a tool to measure dietary and regional effects on the complete profile of extracellular amino acids in the hypothalamus of rats. *Life sciences*, *57*(21), 1911-1923.

16. Savaa, A., Barisonea, I., Maurob, D.D., Neurosci. Lett. 313, 37 (2001)

17. Lütke-Eversloh, T., & Stephanopoulos, G. (2007). L-tyrosine production by deregulated strains of Escherichia coli. *Applied microbiology and biotechnology*, *75*, 103-110.

18. Yang, L., Chen, C., Liu, X., Shi, J., Wang, G., Zhu, L., ... & Doherty, B. E. (2010). Use of cyclodextrin-modified gold nanoparticles for enantioseparations of drugs and amino acids based on pseudostationary phase-capillary electrochromatography. *Electrophoresis*, *31*(10), 1697-1705.

19. Pérez, L., Pinazo, A., García, M. T., Lozano, M., Manresa, A., Angelet, M., . & Infante, M. R. (2009). Cationic surfactants from lysine: Synthesis, micellization and biological evaluation. *European journal of medicinal chemistry*, *44*(5), 1884-1892.

20. Seguer, J., Molinero, J., Manresa, A., & Caelles, J. (1994). Physicochemical and antimicrobial properties of N ″-acyI-L-arginine dipeptides from. *Journal of the Society of Cosmetic Chemists*, *45*, 53-63.

21. Lozano, N., Perez, L., Pons, R., Luque-Ortega, J. R., Fernández-Reyes, M., Rivas, L., & Pinazo, A. (2008). Interaction studies of diacyl glycerol arginine-based surfactants with DPPC and DMPC monolayers, relation with antimicrobial activity. *Colloids and Surfaces A: Physicochemical and Engineering Aspects*, *319*(1-3), 196-203.

22. Singh, H. L., Sharma, M., & Varshney, A. K. (2000). Studies on coordination compounds of organotin (IV) with schiff bases of amino acids. *Sythesis and Reactivity in Inorganic and Matel-Organic Chemistry*, *30*(3), 445-456.

23. Nath, M., Pokharia, S., & Yadav, R. (2001). Organotin (IV) complexes of amino acids and peptides. *Coordination Chemistry Reviews*, *215*(1), 99-149.

24. Refat, M. S., El-Korashy, S. A., & Ahmed, A. S. (2008). Preparation, structural characterization and biological evaluation of L-tyrosinate metal ion complexes. *Journal of Molecular Structure*, *881*(1-3), 28-45.

25. GIBSON, C. J., WATKINS, C. J., & WURTMAN, R. J. (1982). The effects of tyrosine and other nutrients on neurotransmitter synthesis in the brain and retina. *Retina*, *2*(4), 332-340.

26. Zhang, L., Huang, J., Ren, L., Bai, M., Wu, L., Zhai, B., & Zhou, X. (2008). Synthesis and evaluation of cationic phthalocyanine derivatives as potential inhibitors of telomerase. *Bioorganic & medicinal chemistry*, *16*(1), 303-312.

27. He, Y., Wang, Y., Tang, L., Liu, H., Chen, W., Zheng, Z., & Zou, G. (2008). Binding of puerarin to human serum albumin: a spectroscopic analysis and molecular docking. *Journal of Fluorescence*, *18*(2), 433-442.

28. Abbas, M., Saeed, F., Anjum, F. M., Afzaal, M., Tufail, T., Bashir, M. S.,. & Suleria, H. A. R. (2017). Natural polyphenols: An overview. *International Journal of Food Properties*, *20*(8), 1689-1699.

29. Hertog, M. G., Feskens, E. J., Kromhout, D., Hollman, P. C. H., & Katan, M. B. (1993). Dietary antioxidant flavonoids and risk of coronary heart disease: the Zutphen Elderly Study. *The lancet*, *342*(8878), 1007-1011.

30. Serafini, M., Testa, M. F., Villaño, D., Pecorari, M., Van Wieren, K., Azzini, E., ... & Maiani, G. (2009). Antioxidant activity of blueberry fruit is impaired by association with milk. *Free Radical Biology* Agardh, E. E.,

Carlsson, S., Ahlbom, A., Efendic, S., Grill, V., Hammar, N., ... & Östenson, C. G. (2004). Coffee consumption, type 2 diabetes and impaired glucose tolerance in Swedish men and women. *Journal of internal medicine*, *255*(6), 645-652.*and Medicine*, *46*(6), 769-774.

31. Livingstone, K. M., Lovegrove, J. A., & Givens, D. I. (2012). The impact of substituting SFA in dairy products with MUFA or PUFA on CVD risk: evidence from human intervention studies. *Nutrition Research Reviews*, *25*(2), 193-206.

32. Agardh, E. E., Carlsson, S., Ahlbom, A., Efendic, S., Grill, V., Hammar, N., ... & Östenson, C. G. (2004). Coffee consumption, type 2 diabetes and impaired glucose tolerance in Swedish men and women. *Journal of internal medicine*, *255*(6), 645-652.

33. Belay, A. (2011). Some biochemical compounds in coffee beans and methods developed for their analysis. *International Journal of the Physical Sciences*, *6*(28), 6373-6378.

34. Agardh, E. E., Carlsson, S., Ahlbom, A., Efendic, S., Grill, V., Hammar, N., ... & Östenson, C. G. (2004). Coffee consumption, type 2 diabetes and impaired glucose tolerance in Swedish men and women. *Journal of internal medicine*, *255*(6), 645-652.

35. Tuomilehto, J., Hu, G., Bidel, S., Lindström, J., & Jousilahti, P. (2004). Coffee consumption and risk of type 2 diabetes mellitus among middle-aged Finnish men and women. *Jama*, *291*(10), 1213-1219.

36. Ali, M., Keppler, J. K., Coenye, T., & Schwarz, K. (2018). Covalent whey protein–rosmarinic acid interactions: a comparison of alkaline and enzymatic modifications on physicochemical, antioxidative, and antibacterial properties. *Journal of Food Science*, *83*(8), 2092-2100.

37. Zhang, Y., & Zhong, Q. (2012). Binding between bixin and whey protein at pH 7.4 studied by spectroscopy and isothermal titration calorimetry. *Journal of agricultural and food chemistry*, *60*(7), 1880-1886.

38.Tang, B., Huang, Y., Ma, X., Liao, X., Wang, Q., Xiong, X., & Li, H. (2016). Multispectroscopic and docking studies on the binding of chlorogenic acid isomers to human serum albumin: Effects of esteryl position on affinity. Food Chemistry, 212, 434–442

39.Yin, Y., Xie, M., Wu, H., Jiang, M., Zheng, J., & Wei, Q. (2009). Interaction of calcineurin with its activator, chlorogenic acid revealed by spectroscopic methods. Biochimie, 91(7), 820–825.

40.Li, X., & Ni, T. (2016). Probing the binding mechanisms of α-tocopherol to trypsin and pepsin using isothermal titration calorimetry, spectroscopic, and molecular modeling methods. Journal of Biological Physics, 42, 415–434.

41.Li, S., Huang, K., Zhong, M., Guo, J., Wang, W., & Zhu, R. (2010). Comparative studies on the interaction of caffeic acid, chlorogenic acid and ferulic acid with bovine serum albumin. Spectrochimica Acta Part A: Molecular and Biomolecular Spectroscopy, 77(3), 680–686. https://doi.org/10.1016/j.saa.2010.04.026

42.Danciu, C., Soica, C., Oltean, M., Avram, S., Borcan, F., Csanyi, E., Ambrus, R., Zupko, I., Muntean, D., & Dehelean, C. A. (2014). Genistein in 1: 1 inclusion complexes with ramified cyclodextrins: theoretical, physicochemical and biological evaluation. International Journal of Molecular Sciences, 15(2), 1962–1982

43.Zhang, Y., Lu, Y., Yang, Y., Li, S., Wang, C., Wang, C., & Zhang, T. (2021). Comparison of non-covalent binding interactions between three whey proteins and chlorogenic acid: Spectroscopic analysis and molecular docking. Food Bioscience, 41, 101035. https://doi.org/10.1016/j.fbio.2021.101035